Title

Presynaptic mitochondrial morphology in monkey prefrontal cortex correlates with working memory and is improved with estrogen treatment

Journal

Proceedings of the National Academy of Sciences of the United States of America, 111(1)

ISSN

0027-8424

Authors

Hara, Yuko

Yuk, Frank

Puri, Rishi

et al.

Publication Date

2014-01-07

DOI

10.1073/pnas.1311310110

Peer reviewed

Presynaptic mitochondrial morphology in monkey prefrontal cortex correlates with working memory and is improved with estrogen treatment

Yuko Hara[a,b,c], Frank Yuk[a,b,c], Rishi Puri[a,b,c], William G. M. Janssen[a,b,c], Peter R. Rapp[d], and John H. Morrison[a,b,c,e,f,1]

[a]Fishberg Department of Neuroscience, [b]Kastor Neurobiology of Aging Laboratories, [c]Friedman Brain Institute, [e]Department of Geriatrics and Palliative Medicine, and [f]Graduate School of Biomedical Sciences, Icahn School of Medicine at Mount Sinai, New York, NY 10029; and [d]Laboratory of Behavioral Neuroscience, National Institute on Aging, Baltimore, MD 21224

Edited by Floyd Bloom, The Scripps Research Institute, La Jolla, CA, and approved November 15, 2013 (received for review June 13, 2013)

Humans and nonhuman primates are vulnerable to age- and menopause-related decline in working memory, a cognitive function reliant on the energy-demanding recurrent excitation of neurons within Brodmann's Area 46 of the dorsolateral prefrontal cortex (dlPFC). Here, we tested the hypothesis that the number and morphology (straight, curved, or donut-shaped) of mitochondria in dlPFC presynaptic boutons are altered with aging and menopause in rhesus monkeys (*Macaca mulatta*) and that these metrics correlate with delayed response (DR) accuracy, a well-characterized measure of dlPFC-dependent working memory. Although presynaptic bouton density or size was not significantly different across groups distinguished by age or menses status, DR accuracy correlated positively with the number of total and straight mitochondria per dlPFC bouton. In contrast, DR accuracy correlated inversely with the frequency of boutons containing donut-shaped mitochondria, which exhibited smaller active zone areas and fewer docked synaptic vesicles than those with straight or curved mitochondria. We then examined the effects of estrogen administration to test whether a treatment known to improve working memory influences mitochondrial morphology. Aged ovariectomized monkeys treated with vehicle displayed significant working memory impairment and a concomitant 44% increase in presynaptic donut-shaped mitochondria, both of which were reversed with cyclic estradiol treatment. Together, our data suggest that hormone replacement therapy may benefit cognitive aging, in part by promoting mitochondrial and synaptic health in the dlPFC.

toroidal mitochondria | axonal bouton | cognition

Working memory is a type of executive function that involves the storage, organization, and update of information which together guide decision making and goal-directed behavior (1, 2). This complex function is highly vulnerable to age- and menopause-related decline in humans and nonhuman primates and can be assessed in rhesus monkeys using the well-characterized delayed response (DR) test of visuospatial working memory (3–6). Rhesus monkeys are exceptionally valuable models of human aging, menopause, and related cognitive decline, because their brain anatomy, neuronal gene expression, reproductive physiology, and patterns of endocrine senescence closely resemble those of humans (4, 7–10). Importantly, they fail to develop the histopathological features of Alzheimer's disease (11–13). Thus, we can investigate the neurobiological parameters that are coupled to age- and menopause-related cognitive dysfunction in the absence of confounding factors inherent to pathology.

Performance on DR is mediated in part by layer III neurons of the dorsolateral prefrontal cortex (dlPFC) Brodmann's Area 46, which exhibit persistent spatially tuned firing during the delay period of the DR when the spatial position is held in working memory (1, 14). A recent electrophysiological study showed that firing of these "delay cells" in Brodmann's Area 46 is markedly decreased in aged monkeys (15, 16). This loss of firing can be accounted for partly by structural changes that occur with aging and surgical menopause (ovariectomy), both of which are associated with a dramatic loss of the plastic, thin dendritic spines on dlPFC neurons (17, 18). Intriguingly, cyclic estradiol treatment improves cognitive function in aged ovariectomized monkeys while concurrently restoring these thin spines (18). There is evidence for postsynaptic structural and molecular features that promote working memory (15, 18–20), but the contribution of presynaptic morphology has received less attention.

Because the recurrent firing necessary for working memory is highly energy demanding, the prefrontal cortex (PFC) contains more mitochondria than other cortical regions (15, 21). Mitochondria are very dynamic organelles that perform various metabolic functions, including energy production and facilitation of synaptic transmission (22, 23). In neurons, mitochondria are trafficked throughout the dendritic and axonal extents and are more stationary at synaptic sites, where energy demand is especially high (24, 25). Although postsynaptic dendritic spines lack mitochondria, many presynaptic boutons contain them and promote neurotransmission by accelerating recovery from synaptic depression following activity (26). In cell cultures across many tissue types, mitochondrial stressors such as rotenone (an inhibitor of mitochondrial complex I) or hypoxia can induce the formation of donut-shaped mitochondria, which generate increased levels of reactive oxygen species (ROS) (27, 28).

Here, we tested the hypothesis that mitochondrial number and morphology (Fig. 1) in dlPFC presynaptic boutons of female rhesus monkeys are altered with aging and menopause and correlate

Significance

Human and nonhuman primates are vulnerable to age- and menopause-related decline in working memory, a cognitive function reliant on the energy-demanding excitation of prefrontal cortex (PFC) neurons. The number and strength of presynaptic boutons providing inputs to these PFC neurons regulate their excitability. We show that poor working memory in rhesus monkeys is associated with a higher incidence of presynaptic boutons harboring malformed, donut-shaped mitochondria that form abnormally small synaptic contacts. Surgically induced menopause results in working memory impairment and a concomitant increase in presynaptic donut-shaped mitochondria, both of which are reversed by estradiol treatment. Our findings suggest that hormone replacement therapy benefits cognitive aging, in part, by promoting mitochondrial and synaptic health in the PFC.

Author contributions: Y.H., P.R.R., and J.H.M. designed research; Y.H., F.Y., R.P., and W.G.M.J. performed research; Y.H. analyzed data; and Y.H., P.R.R., and J.H.M. wrote the paper.

The authors declare no conflict of interest.

This article is a PNAS Direct Submission.

See Commentary on page 7.

[1]To whom correspondence should be addressed. E-mail: John.Morrison@mssm.edu.

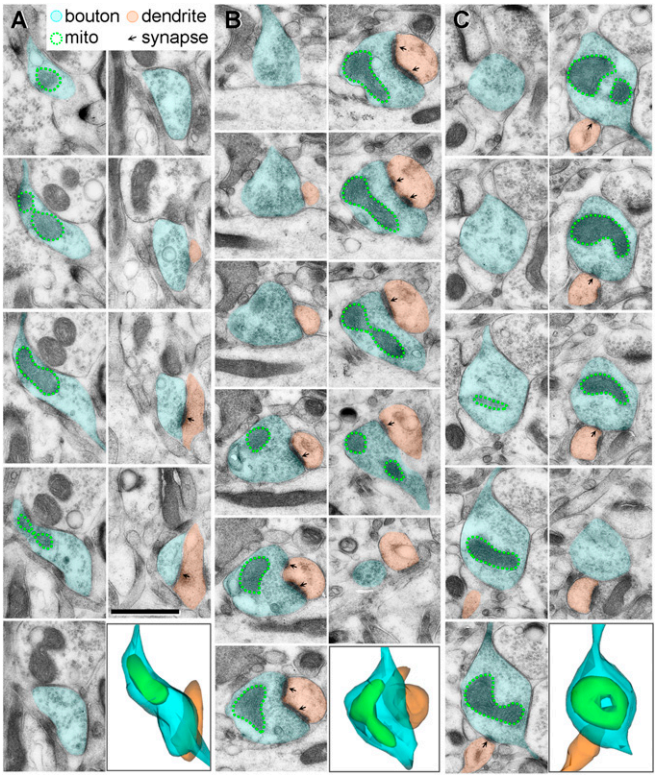

Fig. 1. 3D reconstructions of serial electron micrographs displaying straight (*A*), curved (*B*), and donut-shaped (*C*) mitochondria within monkey dlPFC axonal boutons. (Scale bar: 1 μm.)

with DR accuracy. In addition, we used a cyclic estradiol manipulation known to improve working memory to test whether mitochondrial morphology is regulated in relation to the treatment.

Results

Behavioral Characterization. Behavioral findings for a subset of monkeys (11 of 21) examined in the current experiments are described elsewhere (17). Briefly, contrary to previous reports (3, 5), the results from DR in this cohort of surgically intact monkeys were atypical, showing an overall lack of statistically significant age- or menses-related effects in both acquisition (at 0- and 1-s delay intervals; $P > 0.05$) and delay accuracy (across delay intervals of 5–60 s; $P > 0.05$; Fig. 2 *A* and *B*), despite substantial numerical trends toward impairment with aging and menopause. This lack of effect was caused in part by large within-group variance and the overall poorer than expected performance of young subjects compared with previous studies (3, 5).

On the other hand, the results from a delayed nonmatching-to-sample (DNMS) test of medial temporal lobe-mediated recognition memory were consistent with previous studies (5, 6). Significant group effects were observed in both the number of trials needed to learn the nonmatching-to-sample rule [$F_{(2, 36)} = 9.459$; $P = 0.002$; observed power = 0.955] and recognition accuracy across longer retention intervals [$F_{(2, 36)} = 13.266$; $P = 0.0003$; observed power = 0.992] (Fig. 2 *C* and *D*). Tukey's post hoc tests confirmed that, compared with young adults, aged pre- and peri/postmenopausal monkeys required more trials to acquire the task ($P = 0.009$ and 0.002, respectively) and performed worse at longer delay intervals ($P = 0.001$ for both).

Effects of Aging and Menopause on Presynaptic Mitochondria in the Monkey dlPFC. Because recurrent firing of dlPFC neurons is critical for working memory, we examined whether presynaptic inputs to these neurons and their mitochondrial content are altered with natural aging or menopause. Although ANOVA failed to reveal group effects on the size and density (Fig. 2*E*) of dlPFC axonal boutons ($P > 0.05$), the percentage of boutons that contained mitochondria was reliably different among groups [$F_{(2, 36)} = 5.561$; $P = 0.013$; observed power = 0.788] (Fig. 2*F*), with higher percentages in aged peri/postmenopausal monkeys than in either young ($P = 0.016$) or aged premenopausal

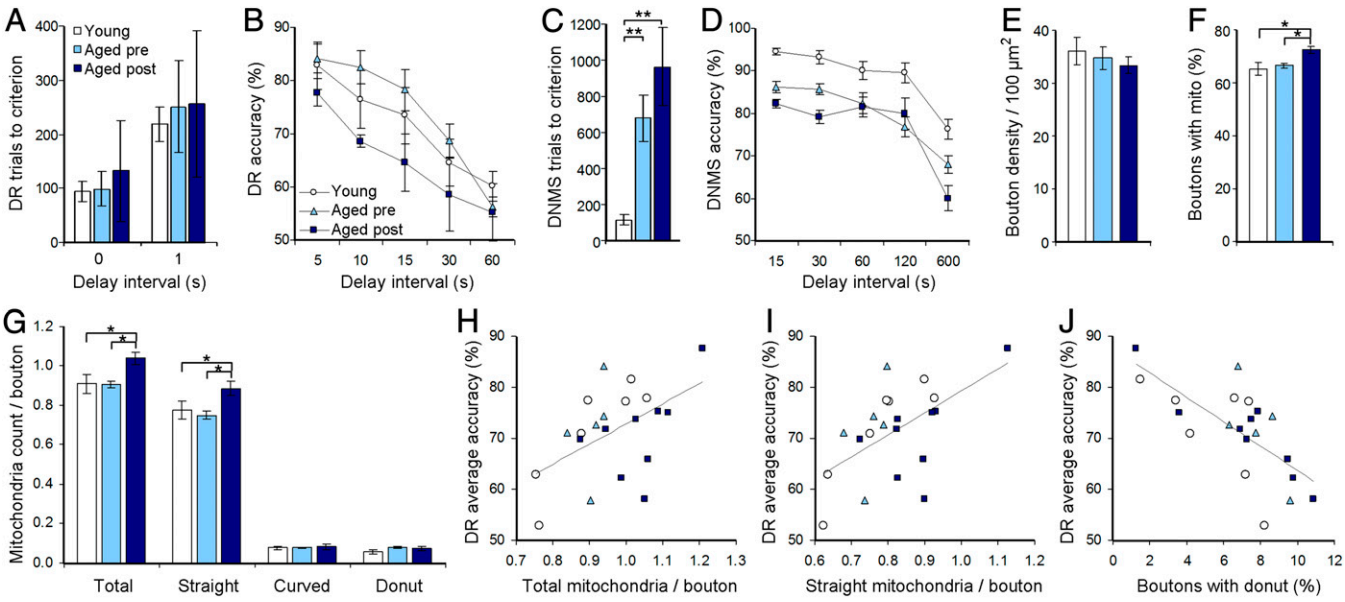

Fig. 2. Behavioral and morphological measures across age and menses status groups. (*A*) Number of trials to reach the DR acquisition criterion at 0- and 1-s delay. (*B*) DR accuracy across delay intervals of 5–60 s. (*C*) Number of trials needed to reach the DNMS acquisition criterion at 10-s delay. (*D*) DNMS accuracy across delay intervals of 15–600 s. (*E*) Axonal bouton density in the dlPFC. (*F*) Percentages of dlPFC boutons containing mitochondria. (*G*) Number of total, straight, curved, and donut-shaped mitochondria per bouton. (*H* and *I*) Positive correlations between the number of total (*H*) and straight (*I*) mitochondria per dlPFC bouton and DR delay accuracy. (*J*) Inverse correlation between the frequency of dlPFC boutons containing donut-shaped mitochondria and DR accuracy. Young, $n = 7$; aged premenopausal, $n = 5$, aged peri/postmenopausal, $n = 9$. $^*P < 0.05$; $^{**}P < 0.01$. Data are expressed as mean ± SEM.

monkeys ($P = 0.032$). Aged peri/postmenopausal monkeys also had a higher number of total mitochondria per bouton than did young ($P = 0.016$) and aged premenopausal ($P = 0.025$) monkeys [$F_{(2, 36)} = 4.674$; $P = 0.023$; observed power = 0.711] (Fig. 2*G*).

Mitochondria are morphologically dynamic and continually undergo fusion and fission events (23). When mitochondria were classified by their shape [$F_{(2, 36)} = 3.586$; $P = 0.049$; observed power = 0.588], aged peri/postmenopausal monkeys had significantly more straight mitochondria per bouton than did young ($P = 0.049$) or aged premenopausal monkeys ($P = 0.030$), whereas no group effects were observed for curved or donut-shaped mitochondria ($P > 0.05$).

Relationships Between dlPFC Presynaptic Mitochondria and Working Memory. We next examined possible relationships between dlPFC mitochondria and the integrity of working memory, measured as average accuracy of DR across 5- to 60-s delay intervals. Although an overall age- or menses-related effect was absent for DR accuracy in this cohort, the wide variability of cognitive performance in young and aged monkeys allowed testing of potential neurobiological parameters that are coupled to individual differences in this function.

The number of total and straight mitochondria per dlPFC presynaptic bouton showed significant positive correlations with DR accuracy (Pearson correlation; total, $n = 21$; total, $r = 0.505$, $P = 0.019$; straight, $r = 0.563$, $P = 0.008$; Fig. 2 *H* and *I*). In striking contrast, the percentage of boutons containing donut-shaped mitochondria, a morphological correlate of metabolic stress (27), exhibited a significant inverse correlation with DR accuracy ($n = 21$; $r = -0.704$, $P = 0.0004$; Fig. 2*J*). This inverse correlation with donut-shaped mitochondria also was significant when the analysis was confined to the aged monkeys ($n = 14$; $r = -0.805$, $P = 0.001$) but failed to reach significance within the young group ($P = 0.11$). All other axonal and mitochondrial measures failed to correlate with DR accuracy ($P > 0.05$ for all).

Notably, none of the dlPFC mitochondrial measures correlated with performance on tasks that require medial temporal lobe integrity (DNMS delay accuracy and object discrimination accuracy; $P > 0.05$ for both), suggesting that the observed correlations are selective for dlPFC function.

Effect of Cyclic Estradiol on dlPFC Presynaptic Mitochondria. Last, we used an intervention known to improve working memory to test experimentally the proposal that mitochondrial morphology is regulated in relation to the treatment. In aged ovariectomized monkeys, cyclic estradiol replacement not only improves working memory compared with vehicle treatment (5) but also increases a class of highly plastic thin spines (17). Additionally, estrogen improves cerebral metabolic rate and blood flow while reducing oxidative stress (29, 30). As previously shown using some of the ovariectomized (OVX) monkeys included here (5), repeated-measures ANOVA confirmed that estradiol treatment significantly improved DR accuracy in aged monkeys [$F_{(1, 7)} = 32.572$; $P = 0.001$; observed power = 0.997] (Fig. 3*A*). The percentage of boutons containing mitochondria and the number of total, straight, and curved mitochondria per bouton were similar between the vehicle (OVX+V)- and estradiol-treated (OVX+E) groups ($P > 0.05$; Fig. 3*B*). The numbers of total and straight mitochondria per bouton in both the OVX+V (total, 0.89 ± 0.06; straight, 0.68 ± 0.04) and OVX+E (total, 0.92 ± 0.04; straight, 0.72 ± 0.06) groups were within the range of surgically intact young (total, 0.91 ± 0.05; straight, 0.78 ± 0.04) and aged premenopausal

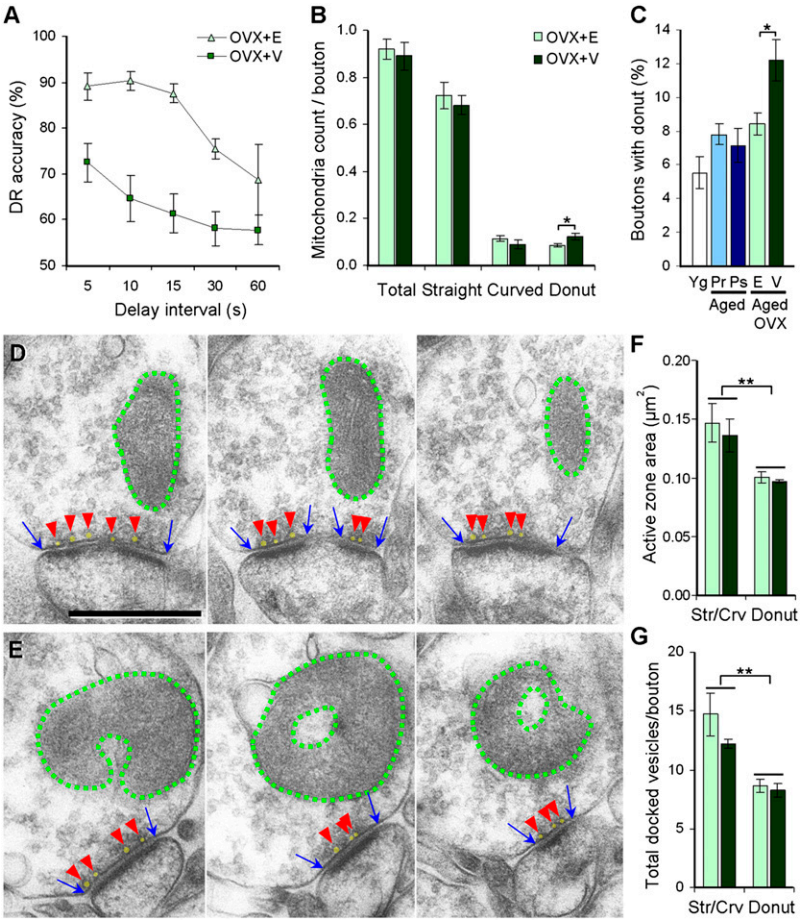

Fig. 3. Estradiol effects on working memory and dlPFC presynaptic mitochondria in aged ovariectomized monkeys. (*A*) DR accuracy across 5- to 60-s delay intervals in aged ovariectomized monkeys treated with vehicle (OVX+V) or estradiol (OVX+E). (*B*) Number of total, straight, curved, and donut-shaped mitochondria per dlPFC bouton. (*C*) Percentage of dlPFC boutons containing donut-shaped mitochondria. Data from surgically intact young (Yg), aged premenopausal (Aged Pr), and aged peri/postmenopausal (Aged Ps) monkeys are plotted together for reference. (*D* and *E*) Serial electron micrographs of boutons containing straight (*D*) or donut-shaped (*E*) mitochondria. Dotted green lines outline mitochondria, blue arrows indicate the extent of the active zone, and red arrowheads point to docked vesicles, shaded in yellow. (Scale bar: 500 nm.) (*F* and *G*) Size of the active zone and number of docked vesicles in dlPFC boutons plotted by presynaptic mitochondrial morphology. Boutons containing donut-shaped mitochondria exhibited significantly smaller active zone areas (*F*) and fewer docked vesicles (*G*) than boutons containing straight or curved mitochondria. *$P < 0.05$; **$P < 0.01$. Data are expressed as mean ± SEM. Aged OVX+V, $n = 4$; aged OVX+E, $n = 4$; young, $n = 7$; aged premenopausal, $n = 5$; aged peri/postmenopausal, $n = 9$.

monkeys (total, 0.91 ± 0.02; straight, 0.75 ± 0.02) and did not reach the high levels observed in aged peri/postmenopausal monkeys (total, 1.04 ± 0.03; straight, 0.89 ± 0.04).

In contrast, significant treatment effects were observed in the number of donut-shaped mitochondria per bouton [$F_{(1,\ 7)}$ = 6.590; P = 0.043; observed power = 0.575; Fig. 3*B*] and in the percentage of boutons containing donut-shaped mitochondria [$F_{(1,\ 7)}$ = 7.288; P = 0.036; observed power = 0.617] (Fig. 3*C*). The number and frequency of donut-shaped mitochondria in the OVX+V group were 42% and 44% higher, respectively, than in the OVX+E group, which had values within the range of surgically intact aged monkeys (Fig. 3*C*).

Lipofuscin is an autofluorescent accumulation of nondegradable material composed primarily of oxidatively damaged proteins and membrane lipids that, in turn, generate increased levels of ROS (31). Although not specific to presynaptic boutons, general oxidative damage in Area 46 layer III was assessed using lipofuscin fluorescence intensity. Consistent with known antioxidant effects of estradiol (30, 32), lipofuscin intensity was 21% greater in the OVX+V group (arbitrary units per pixel: 9.37 ± 0.80) than in the OVX+E group (7.74 ± 0.24) group [$F_{(1,\ 7)}$ = 4.219; P = 0.061].

Finally, we explored whether donut-shaped mitochondria in axonal boutons were associated with dysfunctional synapses. Regardless of treatment ($P > 0.05$), boutons harboring donut-shaped mitochondria exhibited a smaller active zone area [$F_{(1,\ 7)}$ = 15.32; P = 0.004; observed power = 0.927] and fewer docked synaptic vesicles [$F_{(1,\ 7)}$ = 23.75; P = 0.001; observed power = 0.988] than seen in boutons containing straight or curved mitochondria (Fig. 3 *D*–*G*). Bouton size was similar across mitochondrial shapes ($P > 0.05$) and did not drive the observed differences in active zone area or docked vesicle counts. Therefore, boutons harboring donut-shaped mitochondria formed smaller synapses and had fewer readily releasable synaptic vesicles than those containing straight or curved mitochondria.

Discussion

This study links mitochondrial number and morphology with working memory performance. Working memory in rhesus monkeys correlated positively with the number of total and straight mitochondria in dlPFC presynaptic boutons. In contrast, it correlated inversely with the frequency of boutons harboring donut-shaped mitochondria, which formed smaller synaptic contacts and had fewer readily releasable vesicles. The abrupt loss of estrogen by ovariectomy increased the incidence of presynaptic donut-shaped mitochondria, and cyclic estradiol treatment reversed this increase to levels comparable to those in ovary-intact aged monkeys. Together, these findings suggest that hormone replacement therapy may improve working memory, in part by promoting mitochondrial and synaptic health in the dlPFC.

Mitochondrial Changes with Aging and Menopause. Regardless of age or menses status, the great majority (60–80%) of dlPFC axonal boutons contained one or more mitochondria, consistent with the high energy demands of this brain region (15, 21). This level is substantially greater than in the rat hippocampus, where only about 40% of boutons have mitochondria (33).

Aged monkeys that had undergone natural menopause had a higher percentage of boutons containing mitochondria as well as a higher number of total and straight mitochondria per bouton than did either young or aged premenopausal monkeys. These differences were found in the absence of age- or menses-related effects on axonal bouton density and size. Therefore, in contrast to models of neurodegeneration (34, 35), normal aging and natural menopause did not result in overt loss of mitochondria. Instead, the mitochondrial increase observed in aged peri/postmenopausal monkeys may reflect compensatory mechanisms for aging- and menopause-related mitochondrial dysfunction (30). This possibility is compatible with a functional imaging study in humans demonstrating that senior adults require overactivation of Brodmann's Area 46 to achieve working memory performance equivalent to that in young adults (36). The increase also may result from mitochondrial accumulation in presynaptic boutons with aging, because the aged peri/postmenopausal monkeys were significantly older than the premenopausal monkeys. Nevertheless, the findings in aged peri/postmenopausal monkeys provide a possible structural basis for the milder cognitive consequences of natural as compared with surgical menopause (30, 37, 38).

Correlations Between dlPFC Presynaptic Mitochondria and Working Memory. The number of total and straight mitochondria per dlPFC bouton correlated positively with the working memory scores for individual monkeys. In striking contrast, having a higher percentage of presynaptic donut-shaped mitochondria was coupled with worse working memory.

Synaptic mitochondria are not required for basal synaptic transmission, as is consistent with observations that some synaptic boutons completely lack mitochondria (33, 39). However, presynaptic mitochondria are required for neurotransmission during intense stimulation, because mobilization of reserve pool synaptic vesicles is fueled by mitochondrial ATP (39). Thus, our findings linking mitochondrial abundance with working memory are consistent with the high energy requirement for recurrent firing that mediates this function (1, 14, 15).

Although abundant mitochondria sustain intense neurotransmission, this activity is accompanied by an elevation in ROS generation (40). The brain is particularly vulnerable to the effects of oxidative stress because it consumes high amounts of oxygen and expresses lower antioxidant activity than other tissues (41, 42). In nonneuronal cell cultures, conditions that strain mitochondrial function, such as rotenone (a mitochondrial complex I inhibitor) or hypoxia–reoxygenation stress, increase ROS generation and induce the formation of donut-shaped mitochondria via the opening of the permeability transition pore or potassium channels (27, 28). Straight mitochondria produce the lowest levels of ROS, and donut-shaped mitochondria are associated with elevated ROS production (28). Thus, even small increases in ROS-induced formation of donut-shaped mitochondria may cause a positive feedback loop, further increasing ROS production and negatively affecting mitochondrial function. Our data linking presynaptic donut-shaped mitochondria with smaller synaptic contacts and poor working memory are in line with this body of work and suggest that interventions targeted at preventing the formation of donut-shaped may protect against age-related cognitive dysfunction.

Protective Effects of Cyclic Estradiol on dlPFC Mitochondria. Surgical menopause induced by bilateral ovariectomy did not increase the frequency of axonal boutons with mitochondria or the numbers of total or straight mitochondria per bouton, as was seen with natural menopause in aged peri/postmenopausal monkeys.

One key effect seen with ovariectomy in aged monkeys was a 44% increase in the incidence of presynaptic boutons containing donut-shaped mitochondria that were associated with small synaptic contacts and poor working memory. This increase in donut-shaped mitochondria was not seen with natural menopause but was reversed with cyclic estradiol treatment in aged ovariectomized monkeys, suggesting that the abrupt loss of estrogen after ovariectomy has more serious consequences for metabolic functions than natural menopause (43). Indeed, estrogen has many antioxidant effects: It improves mitochondrial efficiency, enhances calcium sequestration in the mitochondria, and reduces ROS formation (30, 32, 44). These effects are likely mediated by the estrogen receptor β, which exerts its actions in both the nucleus and mitochondria and regulates genes involved in mitochondrial electron transport and ROS pathways (45, 46). Together with evidence suggesting that antioxidant pretreatment prevents the formation of donut-shaped mitochondria and ROS

production (28), estradiol may enhance working memory in part by its antioxidant effects on dlPFC presynaptic mitochondria.

Implications. In the human brain, aging is associated with a significant decline in mitochondrial function and oxidative damage to DNA, proteins, and lipids (47–49). Furthermore, in neurodegenerative diseases, metabolic problems occur long before the onset of neuronal death and cognitive impairment (50, 51). The incidence of donut-shaped mitochondria that was associated with smaller synapses, fewer readily releasable vesicles, and poor working memory was decreased with estradiol treatment in aged ovariectomized monkeys. In addition, a recent study demonstrated that rotenone-induced formation of donut-shaped mitochondria can be prevented by antioxidant pretreatment (28). Thus, early interventions targeted at maintaining healthy mitochondrial structure and function, whether hormonal or antioxidant treatments, may profoundly impact dlPFC and other brain regions that are highly vulnerable to oxidative stress, thereby offering effective protection against age-related cognitive decline.

Materials and Methods

Monkeys. Rhesus monkeys (*Macaca mulatta*; total $n = 29$) were housed in colonies of ~40 individuals at the California National Primate Research Center, University of California, Davis. The average life span of captive rhesus monkeys is under 25 y, and human age equivalence is estimated at a 1:3 ratio (52). Menopause in rhesus monkeys typically occurs by age 27 y, later in life than in humans (10, 53). All experiments were conducted in compliance with the National Institutes of Health *Guide for the Care and Use of Laboratory Animals* (54) and were approved by the Institutional Animal Care and Use Committee at the University of California, Davis.

The surgically intact cohort comprised seven young adult (10.4 ± 0.5 y) and 14 aged (29.0 ± 1.1 y) female rhesus monkeys. None of the monkeys had prior invasive or pharmacological manipulations expected to influence the cognitive or neurobiological measures examined here. Visual inspection for vaginal bleeding was conducted daily for 2 y before perfusion. Normal menses cycle length in young adult rhesus macaques is typically 24–34 d (53). Because vaginal bleeding may have escaped detection in some cases, we adopted a more liberal cycle length criterion of 24–45 d (averaged in the last 12 mo) to classify monkeys as premenopausal; monkeys in which the cycle length exceeded that range were classified as peri/postmenopausal. Ovarian status was confirmed by urinalysis of endocrine data for 16 of the 21 monkeys.

Eight aged females (22 y ± 7 mo) classified as pre- and perimenopausal were ovariectomized bilaterally and randomly assigned to age-matched vehicle (OVX+V, $n = 4$) and estradiol (OVX+E, $n = 4$) groups, as described in detail previously (5). Monkeys were injected with ketamine (10 mg/kg, i.m.) and atropine (0.04 mg/kg, s.c.), intubated, and placed on isoflurane anesthesia. After a ventral midline incision was made, the ovarian vessels and fallopian tubes were isolated, ligated, and severed. The ovaries were removed, and the abdominal wall was closed in layers. Animals were observed until responsive, and oxymorphone was administered for postoperative analgesia (1.5 mg/kg, i.m., three times/d for 2 d). After a postovariectomy interval of 30 ± 1.7 wk, 100 μg of estradiol cypionate (Pharmacia) in 1 mL of sterile peanut oil (OVX+E) or 1 mL of peanut oil alone (OVX+V) was injected intramuscularly every 3 wk throughout 2–3 y of behavioral testing. Injections were administered in a blinded manner.

Serum Chemistry. Blood glucose, cholesterol, and triglyceride levels for each monkey were obtained from routine blood tests. None of these values was significantly different across groups (young, aged premenopausal, and aged peri/postmenopausal) or with estradiol treatment ($P > 0.05$). Importantly, these values did not correlate with any of the behavioral or mitochondrial measures ($P > 0.05$), suggesting that findings from this study were not driven by metabolic disturbances associated with hyperglycemia or hyperlipidemia.

Behavioral Testing Procedures. Behavioral testing was not timed with the monkey's menstrual cycle or injections, because each test was carried out daily for several months. The DR test of working memory was conducted as described in detail previously (5). Subjects watched from behind a transparent screen while the left or right well was baited with a food reward. Both wells were covered, and an opaque screen was lowered to impose the retention interval, after which the subject retrieved the reward if the correct location was chosen. During the acquisition phase, the screen was raised immediately (0 s). After the monkey met a criterion of 90% correct or better, it was retested to criterion at a retention interval of 1 s. Successively longer retention intervals of 5, 10, 15, 30, and 60 s then were imposed, increasing working memory demands (90 trials total at each delay, 30 trials/d, intertrial interval = 20 s). The DNMS test of recognition memory and the two-choice object discrimination test were conducted exactly as previously described (5). When perfusion could not be scheduled shortly after completion of behavioral testing, monkeys continued mock testing until the day before perfusion to avoid testing-induced variability in morphological measures.

Perfusion and Tissue Processing. After monkeys were deeply anesthetized with ketamine hydrochloride (25 mg/kg) and pentobarbital (20–35 mg/kg, i.v.), intubated, and mechanically ventilated to prevent hypoxia and ischemia, 1.5 mL of 0.5% sodium nitrate was injected into the left ventricle of the heart, and the descending aorta was clamped. Surgically intact monkeys were perfused transcardially with cold 1% paraformaldehyde in 0.1 M phosphate buffer (PFA/PB; pH 7.2) for 2 min, followed by 4% (wt/vol) PFA/PB for 60 min. Ovariectomized monkeys (OVX+V, OVX+E) were perfused with cold 1% PFA/PB for 1 min, followed by 4% PFA/PB for 12 min. After perfusion, the PFC region spanning the principal sulcus (Brodmann's Area 46) was postfixed for 6 h in 4% PFA/PB with 0.125% glutaraldehyde, washed in PB, and sectioned at 50-μm and 400-μm thicknesses on a vibratome (Leica) for confocal and electron microscopy, respectively.

The 50-μm sections were mounted on glass slides and coverslipped with Vectashield mounting medium (Vector Laboratories). Images of autofluorescent lipofuscin in Brodmann's Area 46 layer III were obtained using a Zeiss LSM 780 inverted microscope (Carl Zeiss) with an Argon 488-nm wavelength set at 2% laser output, a 40×/NA 1.46 objective set to a digital zoom of 0.6×, pixel resolution set to 1,024 × 1,024 (12 Bit), and line averaged four times at a pixel dwell of 3.15 μs. All images were taken at a depth of 10 μm from the tissue surface and were adjusted for similar gain and offset values. Three images from Brodmann's Area 46 layer III (total area of 0.378 mm^2) were taken per animal. Images were imported into Adobe Photoshop version CS5 (Adobe Systems Inc.), and mean lipofuscin intensity per pixel was calculated as the average of the three raw images, subtracting background intensity (mean intensity of nine blood vessels or nuclei lacking lipofuscin). Freeze substitution and low-temperature embedding of the 400-μm sections were performed exactly as previously described (55). Fifteen or more consecutive ultrathin sections were cut at 80-nm thickness using a Diatome diamond knife (Electron Microscopy Sciences) and were mounted on each formvar/carbon-coated slot grid (Electron Microscopy Sciences). To ensure that images were taken from layer III of Brodmann's Area 46, images were captured 250–350 μm from the intersection of acellular layer I and cell-rich layer II. Fields containing cell bodies and blood vessels were avoided.

Quantitative Analyses of Presynaptic Bouton Characteristics. All imaging and axonal and mitochondrial analyses were performed by the same experimenter, blind to the group designation and behavioral performance of subjects. For each monkey, five series of 15 consecutive ultrathin sections were imaged at 2,500× on an Hitachi H-7700 electron microscope (Hitachi High Technologies America, Inc.) with an AMT Advantage CCD camera (Advanced Microscopy Techniques), using a systematic-random approach. The total volume of Brodmann's Area 46 layer III examined per monkey was 517.84 μm^3. For each series, the middle eighth section was used as a reference, and all axonal boutons containing at least three synaptic vesicles that were transected in this section were identified and analyzed. On average, 150 boutons were analyzed per monkey; each bouton was followed throughout the series, and the number and morphology of mitochondria were recorded. Mitochondria were classified into three shapes: straight, curved, or donut-shaped. Curved mitochondria were bent more than 90°. Donut (toroidal) mitochondria were ring-shaped. All other mitochondria were classified as straight. For synaptic vesicle and active zone measurement, at least 10 boutons per monkey containing donut-shaped mitochondria and 10 boutons per monkey containing straight or curved mitochondria were imaged across 15 serial sections at 10,000×. The synaptic active zone area, immediately apposing the postsynaptic density and exhibiting a darker plasma membrane, was determined by summing the lengths of the active zone across the series and multiplying that figure by the section thickness (80 nm). A vesicle was counted as docked when its membrane overlapped with the active zone membrane. Bouton volumes were estimated as previously described (56). Approximately 92% of all boutons were contained within the 15 serial sections, regardless of age, menses status, or treatment. Boutons extending beyond 15 sections were included in the analyses to avoid preferentially excluding larger boutons. The electron micrographs were adjusted for brightness and sharpness with Adobe Photoshop CS5. 3D reconstructions of a subset of axonal boutons and mitochondria were performed using free software (Reconstruct, version

1.1.0.0; http://synapses.clm.utexas.edu) developed by Kristen Harris and her laboratory (University of Texas at Austin, Austin, TX).

Statistical Analyses. SPSS 20.0 (SPSS Inc.) was used for all statistical analyses. The behavioral and morphological data were not significantly different from a normal distribution (one-sample Kolmogorov–Smirnov test; $P > 0.05$ for all measures); therefore, parametric statistics were used. One-way and repeated-measures ANOVA were used to determine whether cognitive task acquisition and accuracy, respectively, were different across groups designated by age and menses status or by treatment. Behavioral data were plotted based on the classification of menses status at the time of testing. Multivariate ANOVA followed by Tukey's post hoc test was used to probe potential differences in morphological data between groups while correcting for multiple comparisons. Observed power calculations in ANOVA confirmed that the sample size was sufficient to support the data. Axonal and mitochondrial data are expressed based on the classification of menses status at the time of perfusion. Pearson correlations evaluated the relationships between morphological indices and behavioral measures. Because of the risk for overcorrection, Pearson analysis was not corrected for multiple comparisons. However, the number of significant correlations observed ($n = 4$) significantly exceeded that predicted by chance ($n = 0.45$). Correlation statistics were not run for ovariectomized monkeys because of the small sample size. The α level for statistical significance was set at 0.05.

ACKNOWLEDGMENTS. We thank Mary Roberts, Sania Fong, Deborah Kent, Katie Hartley, Sona Santos, Heather McKay, and Anne Canfield at the California National Primate Research Center for their expert technical assistance involving the rhesus monkeys; Dr. Donald Canfield for veterinary support; Susan Fink, Ginelle Andrews, and Shannon Wadsworth for expert technical assistance in tissue processing; and Dr. Gareth John for helpful comments on the manuscript. This work was supported by National Institute on Aging Grants R37 AG06647, R01 AG010606, and P01 AG16765 (to J.H.M.), and in part by the Intramural Research Program of the National Institute on Aging.

1. Goldman-Rakic PS (1995) Cellular basis of working memory. *Neuron* 14(3):477–485.
2. Morrison JH, Baxter MG (2012) The ageing cortical synapse: Hallmarks and implications for cognitive decline. *Nat Rev Neurosci* 13(4):240–250.
3. Bartus RT, Fleming D, Johnson HR (1978) Aging in the rhesus monkey: Debilitating effects on short-term memory. *J Gerontol* 33(6):858–871.
4. Hara Y, Rapp PR, Morrison JH (2012) Neuronal and morphological bases of cognitive decline in aged rhesus monkeys. *Age (Dordr)* 34(5):1051–1073.
5. Rapp PR, Morrison JH, Roberts JA (2003) Cyclic estrogen replacement improves cognitive function in aged ovariectomized rhesus monkeys. *J Neurosci* 23(13):5708–5714.
6. Roberts JA, Gilardi KV, Lasley B, Rapp PR (1997) Reproductive senescence predicts cognitive decline in aged female monkeys. *Neuroreport* 8(8):2047–2051.
7. Loerch PM, et al. (2008) Evolution of the aging brain transcriptome and synaptic regulation. *PLoS ONE* 3(10):e3329.
8. Nichols SM, et al. (2005) Ovarian senescence in the rhesus monkey (Macaca mulatta). *Hum Reprod* 20(1):79–83.
9. Petrides M, Pandya DN (1999) Dorsolateral prefrontal cortex: Comparative cytoarchitectonic analysis in the human and the macaque brain and corticocortical connection patterns. *Eur J Neurosci* 11(3):1011–1036.
10. Walker ML, Herndon JG (2008) Menopause in nonhuman primates? *Biol Reprod* 79(3):398–406.
11. Cork LC (1993) Plaques in prefrontal cortex of aged, behaviorally-tested rhesus monkeys: Incidence, distribution, and relationship to task performance. *Neurobiol Aging* 14(6):675–676.
12. Gearing M, Tigges J, Mori H, Mirra SS (1996) A beta40 is a major form of beta-amyloid in nonhuman primates. *Neurobiol Aging* 17(6):903–908.
13. Kimura N, et al. (2003) Age-related changes of Alzheimer's disease-associated proteins in cynomolgus monkey brains. *Biochem Biophys Res Commun* 310(2):303–311.
14. Funahashi S, Bruce CJ, Goldman-Rakic PS (1989) Mnemonic coding of visual space in the monkey's dorsolateral prefrontal cortex. *J Neurophysiol* 61(2):331–349.
15. Arnsten AF, Wang MJ, Paspalas CD (2012) Neuromodulation of thought: Flexibilities and vulnerabilities in prefrontal cortical network synapses. *Neuron* 76(1):223–239.
16. Wang M, et al. (2011) Neuronal basis of age-related working memory decline. *Nature* 476(7359):210–213.
17. Dumitriu D, et al. (2010) Selective changes in thin spine density and morphology in monkey prefrontal cortex correlate with aging-related cognitive impairment. *J Neurosci* 30(22):7507–7515.
18. Hao J, et al. (2007) Interactive effects of age and estrogen on cognition and pyramidal neurons in monkey prefrontal cortex. *Proc Natl Acad Sci USA* 104(27):11465–11470.
19. Paspalas CD, Wang M, Arnsten AF (2013) Constellation of HCN channels and cAMP regulating proteins in dendritic spines of the primate prefrontal cortex: Potential substrate for working memory deficits in schizophrenia. *Cereb Cortex* 23(7):1643–1654.
20. Wang M, et al. (2013) NMDA receptors subserve persistent neuronal firing during working memory in dorsolateral prefrontal cortex. *Neuron* 77(4):736–749.
21. Chandrasekaran K, et al. (1992) Differential expression of cytochrome oxidase (COX) genes in different regions of monkey brain. *J Neurosci Res* 32(3):415–423.
22. Ivannikov MV, Sugimori M, Llinás RR (2013) Synaptic vesicle exocytosis in hippocampal synaptosomes correlates directly with total mitochondrial volume. *J Mol Neurosci* 49(1):223–230.
23. Youle RJ, van der Bliek AM (2012) Mitochondrial fission, fusion, and stress. *Science* 337(6098):1062–1065.
24. Chang DT, Honick AS, Reynolds IJ (2006) Mitochondrial trafficking to synapses in cultured primary cortical neurons. *J Neurosci* 26(26):7035–7045.
25. Li Z, Okamoto K, Hayashi Y, Sheng M (2004) The importance of dendritic mitochondria in the morphogenesis and plasticity of spines and synapses. *Cell* 119(6):873–887.
26. Billups B, Forsythe ID (2002) Presynaptic mitochondrial calcium sequestration influences transmission at mammalian central synapses. *J Neurosci* 22(14):5840–5847.
27. Liu X, Hajnóczky G (2011) Altered fusion dynamics underlie unique morphological changes in mitochondria during hypoxia-reoxygenation stress. *Cell Death Differ* 18(10):1561–1572.
28. Ahmad T, et al. (2013) Computational classification of mitochondrial shapes reflects stress and redox state. *Cell Death Dis* 4:e461.
29. Eberling JL, Reed BR, Coleman JE, Jagust WJ (2000) Effect of estrogen on cerebral glucose metabolism in postmenopausal women. *Neurology* 55(6):875–877.
30. Henderson VW, Brinton RD (2010) Menopause and mitochondria: Windows into estrogen effects on Alzheimer's disease risk and therapy. *Prog Brain Res* 182:77–96.
31. Terman A, Brunk UT (2006) Oxidative stress, accumulation of biological 'garbage', and aging. *Antioxid Redox Signal* 8(1-2):197–204.
32. Nilsen J, Diaz Brinton R (2003) Mechanism of estrogen-mediated neuroprotection: Regulation of mitochondrial calcium and Bcl-2 expression. *Proc Natl Acad Sci USA* 100(5):2842–2847.
33. Shepherd GM, Harris KM (1998) Three-dimensional structure and composition of CA3—>CA1 axons in rat hippocampal slices: Implications for presynaptic connectivity and compartmentalization. *J Neurosci* 18(20):8300–8310.
34. Kim J, et al. (2010) Mitochondrial loss, dysfunction and altered dynamics in Huntington's disease. *Hum Mol Genet* 19(20):3919–3935.
35. Wang X, et al. (2009) Impaired balance of mitochondrial fission and fusion in Alzheimer's disease. *J Neurosci* 29(28):9090–9103.
36. Cappell KA, Gmeindl L, Reuter-Lorenz PA (2010) Age differences in prefontal recruitment during verbal working memory maintenance depend on memory load. *Cortex* 46(4):462–473.
37. Greendale GA, et al. (2009) Effects of the menopause transition and hormone use on cognitive performance in midlife women. *Neurology* 72(21):1850–1857.
38. Sherwin BB (1988) Estrogen and/or androgen replacement therapy and cognitive functioning in surgically menopausal women. *Psychoneuroendocrinology* 13(4):345–357.
39. Verstreken P, et al. (2005) Synaptic mitochondria are critical for mobilization of reserve pool vesicles at Drosophila neuromuscular junctions. *Neuron* 47(3):365–378.
40. Milton VJ, Sweeney ST (2012) Oxidative stress in synapse development and function. *Dev Neurobiol* 72(1):100–110.
41. Halliwell B (1992) Reactive oxygen species and the central nervous system. *J Neurochem* 59(5):1609–1623.
42. Shulman RG, Rothman DL, Behar KL, Hyder F (2004) Energetic basis of brain activity: Implications for neuroimaging. *Trends Neurosci* 27(8):489–495.
43. Rocca WA, et al. (2007) Increased risk of cognitive impairment or dementia in women who underwent oophorectomy before menopause. *Neurology* 69(11):1074–1083.
44. Nilsen J, Irwin RW, Gallaher TK, Brinton RD (2007) Estradiol in vivo regulation of brain mitochondrial proteome. *J Neurosci* 27(51):14069–14077.
45. Yang SH, et al. (2004) Mitochondrial localization of estrogen receptor beta. *Proc Natl Acad Sci USA* 101(12):4130–4135.
46. O'Lone R, et al. (2007) Estrogen receptors alpha and beta mediate distinct pathways of vascular gene expression, including genes involved in mitochondrial electron transport and generation of reactive oxygen species. *Mol Endocrinol* 21(6):1281–1296.
47. Mecocci P, et al. (1993) Oxidative damage to mitochondrial DNA shows marked age-dependent increases in human brain. *Ann Neurol* 34(4):609–616.
48. Montine TJ, et al. (2002) Lipid peroxidation in aging brain and Alzheimer's disease. *Free Radic Biol Med* 33(5):620–626.
49. Smith CD, et al. (1991) Excess brain protein oxidation and enzyme dysfunction in normal aging and in Alzheimer disease. *Proc Natl Acad Sci USA* 88(23):10540–10543.
50. Arnold B, Cassady SJ, VanLaar VS, Berman SB (2011) Integrating multiple aspects of mitochondrial dynamics in neurons: Age-related differences and dynamic changes in a chronic rotenone model. *Neurobiol Dis* 41(1):189–200.
51. Mosconi L, et al. (2009) FDG-PET changes in brain glucose metabolism from normal cognition to pathologically verified Alzheimer's disease. *Eur J Nucl Med Mol Imaging* 36(5):811–822.
52. Tigges J, Gordon TP, McClure HM, Hall EC, Peters A (1988) Survival rate and life span of rhesus monkeys at the Yerkes regional primate research center. *Am J Primatol* 15:263–273.
53. Gilardi KV, Shideler SE, Valverde CR, Roberts JA, Lasley BL (1997) Characterization of the onset of menopause in the rhesus macaque. *Biol Reprod* 57(2):335–340.
54. Committee on Care and Use of Laboratory Animals (1985) *Guide for the Care and Use of Laboratory Animals* (Natl Inst Health, Bethesda), DHHS Publ No (NIH) 85-23.
55. Hara Y, et al. (2012) Synaptic correlates of memory and menopause in the hippocampal dentate gyrus in rhesus monkeys. *Neurobiol Aging* 33(2):e17–e28.
56. Hara Y, et al. (2011) Synaptic characteristics of dentate gyrus axonal boutons and their relationships with aging, menopause, and memory in female rhesus monkeys. *J Neurosci* 31(21):7737–7744.